247

Copy
RM L53D21

NACA

RESEARCH MEMORANDUM

MEASUREMENTS OF AERODYNAMIC CHARACTERISTICS AT TRANSONIC SPEEDS OF AN UNSWEPT AND UNTAPERED NACA 65-009 AIRFOIL MODEL OF ASPECT RATIO 3 WITH 1/4-CHORD PLAIN FLAP BY THE NACA WING-FLOW METHOD

By Harold I. Johnson

Langley Aeronautical Laboratory
Langley Field, Va.

NATIONAL ADVISORY COMMITTEE
FOR AERONAUTICS

WASHINGTON

June 10, 1953

NATIONAL ADVISORY COMMITTEE FOR AERONAUTICS

RESEARCH MEMORANDUM

MEASUREMENTS OF AERODYNAMIC CHARACTERISTICS AT TRANSONIC SPEEDS OF AN UNSWEPT AND UNTAPERED NACA 65-009 AIRFOIL MODEL OF ASPECT RATIO 3 WITH 1/4-CHORD PLAIN FLAP BY THE NACA WING-FLOW METHOD

By Harold I. Johnson

SUMMARY

A wing-flow investigation was made to determine the lift, pitching-moment, and hinge-moment characteristics of an unswept and untapered NACA 65-009 airfoil model of aspect ratio 3.01 equipped with a 1/4-chord full-span plain flap. The Mach number range was approximately 0.65 to 1.10 and the corresponding Reynolds number range was approximately 0.5×10^6 to 0.9×10^6. The effects of sealing 69 percent of the length of the 1.1-percent-chord flap gap were investigated as were the effects on flap characteristics of adding roughness to the first 5 percent of the airfoil chord.

The maximum unstalled lift coefficient of the model was found to be almost twice as great above $M = 1.0$ as it was below $M = 0.90$. A compressibility phenomenon that apparently is peculiar to fairly thick aerodynamic surfaces was found to occur near $M = 0.95$ at small angles of attack and flap deflections. This phenomenon was made manifest by a large reduction in lift-curve slope, an abrupt forward movement of the aerodynamic center to a position near the leading edge, an abrupt reversal to a strong positive variation of hinge-moment coefficient with angle of attack, and a reduction of flap effectiveness to approximately zero for small deflections. Below $M = 0.90$ the hinge moments due to deflection with gap sealed were about equal to what would be predicted from thin-airfoil theory and above $M = 1.0$ the hinge moments were approximately what would be expected from the concepts of two-dimensional linear supersonic theory. The hinge-moment variations with angle of attack were very nonlinear at subsonic speeds because of gap effects but were fairly linear and strongly negative at supersonic speeds. The effects of sealing the flap gap at subsonic speeds were to increase flap effectiveness, reduce the hinge moments due to deflection, and make more linear the variations of hinge moment with angle of attack. At supersonic speeds the aerodynamic characteristics were nearly the same with gap either sealed or open.

INTRODUCTION

A wing-flow investigation was made to determine the lift, pitching-moment, and hinge-moment characteristics of an unswept and untapered NACA 65-009 airfoil model of aspect ratio 3.01 equipped with a 1/4-chord full-span plain flap. This investigation is closely related to those reported in references 1 to 4 which dealt with an equivalent 35° sweptback model on which full-span flaps having different kinds of aerodynamic balance were investigated at transonic speeds.

By present-day standards, a 9-percent-thick aerodynamic surface of aspect ratio 3 would be considered excessively thick for most applications. Like most wing-flow or tunnel-bump experiments, the Reynolds numbers were low in the present tests (less than 0.9×10^6); in spite of these limitations, the data are thought to be of appreciable interest. In particular, the variation of maximum lift with Mach number, the hinge-moment measurements, and the effects of flap gap at transonic speeds may be of special interest.

SYMBOLS

M	average Mach number over model
q	average dynamic pressure over model
S	total model area
C_L	model lift coefficient, $\frac{\text{Model lift}}{qS}$
c	model chord
$\bar{c}$	model mean aerodynamic chord
C_m	model pitching-moment coefficient measured about axis at 39.5 percent mean aerodynamic chord, $\frac{\text{Model pitching moment about } 0.395\bar{c}}{qS\bar{c}}$
M_f	area moment of flap about hinge line
C_h	model hinge-moment coefficient, $\frac{\text{Model hinge moment}}{2qM_f}$

α	angle of attack
δ	flap deflection
C_{L_α}	variation of model lift coefficient with angle of attack per degree, $\frac{\partial C_L}{\partial \alpha}$
C_{L_δ}	variation of model lift coefficient with flap deflection per degree, $\frac{\partial C_L}{\partial \delta}$
$C_{m_{\alpha_{0.395\bar{c}}}}$	variation of model pitching-moment coefficient about $0.395\bar{c}$ with angle of attack per degree, $\left(\frac{\partial C_M}{\partial \alpha}\right)_{0.395\bar{c}}$
$C_{m_{\delta_{0.395\bar{c}}}}$	variation of model pitching-moment coefficient about $0.395\bar{c}$ with flap deflection per degree, $\left(\frac{\partial C_m}{\partial \delta}\right)_{0.395\bar{c}}$
C_{h_α}	variation of flap hinge-moment coefficient with angle of attack per degree, $\frac{\partial C_h}{\partial \alpha}$
C_{h_δ}	variation of flap hinge-moment coefficient with flap deflection per degree, $\frac{\partial C_h}{\partial \delta}$
$\frac{\partial \alpha}{\partial \delta}$	flap relative effectiveness, $\frac{\partial C_L/\partial \delta}{\partial C_L/\partial \alpha}$
A	aspect ratio
φ	included trailing-edge angle of flap, deg ($\varphi = 6^\circ$)

APPARATUS AND TESTS

The semispan wing-flow model simulated a wing or tail surface of aspect ratio 3.01, taper ratio 1.0, and sweepback angle of 0°. The model was machined from solid beryllium-copper to the contour of the NACA 65-009 section and incorporated a 1/4-chord plain flap mounted on two hinges. The model had a 0.040-inch-thick end plate with a diameter

equal to the chord affixed to its root in order that proper semispan testing conditions would be more nearly realized. A photograph of the model with end plate attached is given in figure 1, and a drawing, including principal dimensions, is given in figure 2. The model (fig. 1) had two flush removable plates between the hinges to provide for installation of a thin sheet-rubber gap seal. The length of gap sealed was 69 percent of the hinge-line length for the gap-sealed condition and, for the gap-open condition, the gap width was 1.1 percent of the airfoil chord. It should be noted that the gap was unusually large. The model was mounted on a strain-gage balance located inside the wing of a North American F-51D wing-flow airplane in such a way that the pitching moments were measured about an axis at 39.5 percent of the model mean aerodynamic chord.

Measurements were made of the lift, pitching moment, and hinge moment for an angle-of-attack range from about -5° to 30°, a flap-deflection range of about -12° to 22°, and a Mach number range from about 0.65 to 1.10. The measurements of maximum lift were limited to $M = 1.05$ for reasons to be discussed subsequently. The approximate Reynolds numbers existing during the tests are shown as a function of Mach number in figure 3. Some tests were made with a layer of 0.003- to 0.005-inch Carborundum particles affixed to the first 5 percent chord on both upper and lower surfaces of the model. These roughness tests were made only for the case of variable flap angle with the model set for 0° angle of attack. No corrections were made for the effects of aeroelasticity in view of the extreme ruggedness of the model and the relatively low dynamic pressures encountered at the test altitude range of from approximately 30,000 feet to 18,000 feet. Further details concerning instrumentation, test technique, and probable accuracies can be found in references 1 to 4.

RESULTS AND DISCUSSION

Characteristics in Angle of Attack

The variations of lift, pitching-moment, and hinge-moment coefficients with angle of attack at 0° flap deflection are shown in figure 4 for increments in Mach number of 0.05 over the speed range tested.

Perhaps the most striking feature shown by the lift measurements (fig. 4(a)) is the extremely large increase in maximum lift coefficient that occurred just prior to the attainment of sonic velocity. The values of $C_{L_{max}}$ and of angle of attack, read either at the peaks in the lift curves or slightly beyond the occurrence of an abrupt decrease in lift-curve slope (in cases where no definite peak existed), are plotted

against Mach number in figure 5. Comparison of these data with those of references 1 and 4 indicate that 35° sweptback models tested under the same conditions gave higher maximum lift coefficients at Mach numbers below 0.97 and lower maximum lift coefficients above this Mach number. The low maximum lift coefficients found in the subsonic speed range are believed to be due largely to the low Reynolds numbers as well as to the low aspect ratio and relatively small leading-edge radius of the 65-009 airfoil section; however, it is unlikely that the large increase in maximum lift with increasing Mach number would be eliminated by an increase in Reynolds number. Above a Mach number of 1.05 it became impossible to measure maximum lift coefficients inasmuch as the pressures set up by the wing-flow model caused the flow field about the right wing of the wing-flow airplane to change radically in an abrupt manner. When this happened, the airplane was subjected to a rather violent rolling oscillation which had a frequency exactly twice that of the forced oscillations of the wing-flow model. Whenever the model reached either high positive or negative angles of attack, the model lift trace showed a sharp discontinuity and the airplane accelerometer showed losses in normal acceleration of about 1 g during a 4g pull-out which represented losses in airplane lift of the order of 8,000 pounds. These losses in lift coincided with the occurrence of right-wing heaviness; therefore, the model constituted an extremely effective spoiler at airplane Mach numbers approaching the maximum permissible (M = 0.75). This phenomenon apparently establishes a limit on the ranges for which techniques such as the wing-flow method can be used to investigate maximum lift. The phenomenon also reemphasizes the possible injurious effects of small protuberances at transonic speeds.

The effect of the flap gap was to decrease the maximum lift coefficient by a small amount over the entire speed range. The effect of the gap on the lift-curve slope was very small and inconsistent over the speed range.

The only other lift characteristic requiring comment occurred over a small angle-of-attack range at $\alpha \approx 0^\circ$ at $M = 0.95$ where the lift-curve slope suffered a decrease. Although not particularly significant in itself, as will be shown later, this very minor change in lift was accompanied by violent changes in hinge-moment characteristics and aerodynamic-center location.

The pitching-moment curves (fig. 4(b)) require little comment. In general, the model showed reasonably constant stability up to the initial stall and at higher angles of attack became more stable. As evidenced by the near-zero values of pitching-moment coefficient at extreme angles of attack, the center of pressure at these angles of attack was in the neighborhood of 40 percent mean aerodynamic chord or somewhat farther back at Mach numbers above 0.85. Except for the sharp decrease in

stability at $M = 0.95$ near $\alpha = 0^\circ$ which will be discussed later, the model became more stable at small angles of attack as the Mach number was increased from subsonic to supersonic values. The latter trend is, of course, to be expected.

The hinge-moment measurements (fig. 4(c)) show several interesting points. As mentioned previously, a violent change in hinge-moment characteristics occurred in the neighborhood of $M = 0.95$ at $\alpha = 0^\circ$. The onset and disappearance of this change is documented in figure 6 which shows the hinge-moment characteristics for small increments in Mach number between 0.90 and 1.0. The reversal in hinge moment is seen to be most severe between Mach numbers of 0.96 and 0.97. Inasmuch as the total lift on the model was only slightly affected, it may be concluded that nearly all the abrupt change in flow characteristics occurred near the trailing edge of the model. Further support for this conclusion was given by the pitching-moment and flap-effectiveness measurements, respectively, which, as will be shown subsequently, indicated that the aerodynamic center moved rapidly forward to a position near the leading edge of the model and the flap effectiveness for small deflections became essentially zero at the same Mach numbers that the flap-floating tendency reversed from with the wind to against the wind.

The flow phenomenon which caused all the foregoing undesirable characteristics appears to be the same as that found by several other investigators (for example, refs. 5 and 6). Göthert (ref. 5) gives a reasonable explanation of the phenomenon based on pressure-distribution measurements and Hemenover and Graham (ref. 6) show schlieren photographs of the flow that substantiate the remaining necessary assumptions made by Göthert. The mechanism of the flow phenomenon may be described briefly as follows:

Consider a symmetrical airfoil at zero angle of attack having a 1/4-chord flap at 0° deflection in a stream of, say, Mach number = 0.95. This airfoil, if of conventional shape, will have a compression shock on the upper surface and one also on the lower surface at the same chordwise station which probably will be close to the hinge line. The pressure on both surfaces will suddenly become higher in going from ahead of, to behind the shock waves, and, if the airfoil is sufficiently thick, there will be partial flow separation starting from the base of the shock waves. Consider now a small positive increase in angle of attack with the flap held at 0° deflection. On the bottom surface the shock wave will move back and tend to become weaker and the partial separation may be reduced. On the upper surface, however, the shock wave will move forward and become slightly stronger and, because of the extremely critical state of the flow equilibrium, the partial separation may be increased to a more extensive flow separation accompanied by a somewhat larger increase in pressure through the upper-surface shock wave. The forward and rearward movements of the shock waves on the upper and lower surfaces,

respectively, together with the differences in pressure rise through the shock waves on the two surfaces, leads to a higher net pressure on the flap upper surface than on the flap lower surface; this accounts for the tendency of the flap to float against the relative wind, accounts for the decrease in lift-curve slope, and also accounts for the large forward movement of the aerodynamic center. Turn now to the case of flap deflection at 0° angle of attack. Assume the flap is given a slight positive deflection. Again, the partial separation on the lower surface tends to be relieved. In this case, however, the abrupt turn in flow of the stream (which is locally supersonic for some distance ahead of the shock wave) produced by the deflected flap causes the pressure to increase on the lower surface of the flap according to expectation. This change is in the correct direction to produce positive flap effectiveness. On the upper surface, however, the separation again increases, the pressure rise through the shock wave again increases, and the flow apparently does not expand around the corner produced by the deflected flap. In the present case these pressure changes resulted in approximately zero change in net lift on the airfoil and therefore the flap effectiveness became essentially zero for small deflections. These separation effects are obviously highly nonlinear because neither the large positive floating tendency nor the zero flap effectiveness extends over very large ranges of angle of attack or flap deflection, respectively. As the Mach number increases to 1.0, the compression shocks on the airfoil move back to the trailing edge so that shock-induced separation can no longer occur.

Inasmuch as the foregoing phenomenon is associated with boundary-layer-flow separation, the magnitude and exact details of the aerodynamic force changes would be expected to depend strongly on Reynolds number. Experience with the Bell X-1 research airplane (ref. 7) seems to indicate that the basic phenomenon occurs also at full scale, at least on the horizontal tail of this airplane. Göthert predicted that the flow breakdown would occur at higher stream Mach numbers for a horizontal tail on an airplane because of the slowing up of the stream caused by the passage of the wing through the air in front of the tail. The data for the X-1 airplane (ref. 7) tend to bear out this prediction. In general, the transonic-flow breakdown under discussion is believed to occur only on airfoil surfaces of fairly large thickness ratio and, probably, of relatively low sweepback inasmuch as no evidence was found of its existence in the investigation of thinner unswept wings in references 8 and 9 nor in the several investigations of 7.4-percent-thick 35° sweptback models reported in references 1 to 4. In this connection it should be remembered that on wings of large sweepback the spanwise-flow effects are very important and that these effects may change the nature of the transonic-flow breakdown entirely.

Returning now to figure 4(c), it may be noted that the hinge-moment variations with angle of attack at subsonic speeds were affected greatly by the presence of the flap gap at small angles of attack. Opening the

gap caused the hinge-moment variations to become erratic and highly nonlinear at small angles of attack. At supersonic speeds, however, there was no measureable effect of the large gap on the hinge-moment variations. The negative flap floating tendency (evidenced by the slopes of the curves) was much stronger at supersonic speeds than at subsonic speeds in accordance with expectation; also, the negative floating tendency above $M = 1.0$ was greater for this unswept model than for the 35° sweptback models of references 1 to 4.

Characteristics in Flap Deflection

The variations in lift, pitching-moment, and hinge-moment coefficients with flap deflection are shown in figure 7 for increments in Mach number of 0.05 over the range tested.

The variations of lift with flap deflection (fig. 7(a)) were reasonably linear over the deflection range tested except at $M = 0.95$ where the flap was practically ineffective for small deflections at $\alpha \approx 0°$; at an angle of attack of 5°, the ineffective deflection range appeared at $\delta \approx -5°$. The reasons for the existence of these characteristics have already been discussed. At subsonic speeds, the addition of roughness caused a slight decrease in flap effectiveness, probably because of an increase in boundary-layer thickness, and the removal of the gap seal caused an appreciable loss in effectiveness, probably because of the tendency for pressure equalization to occur across the gap. Above $M = 1.0$, neither roughness nor leakage through the gap had very much effect on flap lift effectiveness.

Although leakage through the gap caused an appreciable decrease in flap lift effectiveness at subsonic speeds, the data of figure 7(b) indicate that the pitching-moment-producing ability of the flap was slightly increased. These results are explainable on the grounds that flow through the flap gap causes the center of pressure of the flap lift to move rearward appreciably. Another interesting point is that the pitching-moment variation with flap deflection did not go to zero for small flap deflections at $M = 0.95$ even though the lift variation did go to zero in the gap-sealed condition. This point is largely of academic interest in connection with horizontal-tail effectiveness, however, inasmuch as the important change in trimming moment from a horizontal tail arises from its direct lift change rather than from any small change in pitching moment about the tail aerodynamic center due to elevator movement; the latter effect is often disregarded in static stability analyses.

The hinge moments due to deflection (fig. 7(c)) were always great and, for the gap-sealed configuration, were generally of the magnitude expected for an unbalanced flap at either subsonic or supersonic speeds. At $M = 0.95$ where the flap effectiveness was essentially zero for small

deflections, the hinge moments showed some decrease but, as in the case of pitching moments, did not reduce to zero. Over large deflection ranges, the open-gap configuration generally had the greatest hinge moments and the gap-sealed-plus-roughness configuration had the least hinge moments. Here, again, the effect of leakage through the gap is indicated to be a rearward movement of the flap center of pressure which is apparently more important than the lift decrease due to gap leakage insofar as the hinge moments are concerned.

Aerodynamic Parameters at $\alpha = 0^\circ$ and $\delta = 0^\circ$

Aerodynamic parameters measured at 0° angle of attack and 0° flap deflection (instantaneous slopes) are presented in figure 8. Figure 8(a) shows the airfoil and flap absolute lift effectiveness; figure 8(b) shows the flap relative effectiveness; figure 8(c) shows the airfoil and flap pitching-moment parameters related to the axis about which pitching moments were measured; figure 8(d) shows the positions of the center of pressure due to angle of attack (aerodynamic center) and that due to flap deflection (c.p. due to δ), and figure 8(e) shows the hinge-moment parameters with respect to angle of attack and flap deflection. In figure 8(a) the subsonic lift-curve slopes are compared with the theory of reference 10.

A word of caution is believed necessary in regard to figure 8. These data strictly apply only at very small angles of attack and flap deflections. An airplane designed for supersonic speeds might traverse the transonic speed range at angles of attack large enough and, possibly, with elevator deflections such that the extreme changes in aerodynamic parameters shown by figure 8 for Mach numbers between 0.90 and 1.00 would be avoided because, as noted previously, these changes occurred only at low angles of attack and for small ranges of flap deflection. Above $M = 1.0$ and below $M = 0.90$ the parameters shown are reasonably representative of characteristics over fairly large ranges of angle of attack or flap deflection except for the hinge-moment variations with angle of attack below $M = 0.90$ which, as pointed out previously, were highly nonlinear because of gap effects.

In figure 8(a), good agreement is shown between measured and calculated subsonic lift-curve slopes in spite of the low Reynolds numbers. Also, it was found that if the flap absolute effectiveness C_{L_δ} at the lowest test speeds is corrected by linear extrapolation to the case for the gap completely sealed (conditions shown in fig. 8(a) were 0 and 69 percent of hinge-line length sealed), very good agreement is also obtained between measured flap effectiveness and predicted three-dimensional flap effectiveness based on incompressible thin-airfoil theory $\left(C_{L_\delta} = 0.0327\right)$. In figure 8(b) it may be noted that at $M > 1.0$ the flap relative effectiveness is approximately 0.22. As is well known,

the two-dimensional linear-supersonic-theory value of $\partial\alpha/\partial\delta$ for a 1/4-chord flap is 0.25. In figure 8(d) it is seen that the center of pressure due to flap deflection at subsonic speeds is considerably farther rearward with gap open than with the gap partially sealed; this fact has been discussed previously. At $M > 1.0$ the center of pressure due to flap deflection is in close proximity to 87.5 percent of the chord which is the location predicted for a 1/4-chord flap by the two-dimensional linear supersonic theory which neglects aspect ratio and viscosity effects. As is well known, the two-dimensional linear supersonic theory predicts a uniform pressure distribution over the flap and no change in pressures ahead of the flap hinge line due to flap deflection. For such a pressure distribution, it can easily be shown that $C_{h_\delta} = -2C_{L_\delta}$ for a 1/4-chord flap. Reference to figures 8(a) and 8(e) shows that, in the present tests of the model with smooth surface at $M > 1.0$, C_{L_δ} was approximately equal to 0.013 and C_{h_δ} was approximately equal to -0.027 so that the relation $C_{h_\delta} = -2C_{L_\delta}$ was almost exactly satisfied. Therefore, it is implied by the present tests that the pressure distribution on the flap due to flap deflection became essentially uniform soon after a Mach number of 1.0 was exceeded. Finally, figure 8(d) shows that the rearward transonic aerodynamic-center shift was, neglecting the abrupt forward movement at small angles of attack between $M = 0.9$ and 1.0, about 16 percent of the mean aerodynamic chord. This value is about the same as that found from the tests reported in references 1 to 4 of 35° sweptback models of the same aspect ratio and taper ratio.

CONCLUSIONS

Wing-flow tests at Mach numbers between 0.65 and 1.10 of an unswept and untapered NACA 65-009 airfoil model of aspect ratio 3.01 having a 1/4-chord full-span plain flap indicated the following conclusions:

1. The maximum unstalled lift coefficient was almost twice as great above $M = 1.0$ as it was below $M = 0.90$.

2. A compressibility phenomenon apparently peculiar to fairly thick aerodynamic surfaces was found in the region of $M = 0.95$ for small angles of attack and flap deflections. Evidences of this phenomenon were a large reduction in lift-curve slope, an abrupt forward movement of the aerodynamic center to a position near the leading edge, an abrupt reversal to a strong positive variation of hinge-moment coefficient with angle of attack, and a reduction of flap effectiveness to essentially zero for small flap deflections.

3. The hinge-moment variation with flap deflection with gap sealed had large negative values of about the magnitude predicted by thin-airfoil theory at speeds below $M = 0.90$ and of about the magnitude expected from the concepts of two-dimensional linear supersonic theory at Mach numbers above 1.0. The hinge-moment variations with angle of attack were very nonlinear at subsonic speeds because of gap effects but were fairly linear and had large negative values at $M > 1.0$.

4. The effects of sealing 69 percent of the length of the 1.1-percent-chord flap gap were to increase the flap lift effectiveness appreciably, to move the center of pressure due to flap deflection forward appreciably (with a consequent reduction in hinge moment due to deflection), and to increase the linearity of the hinge-moment variations with angle of attack, at speeds below $M = 0.90$; at supersonic speeds, sealing the flap gap had little effect on any of the measured aerodynamic parameters. Sealing the gap increased the maximum lift coefficient slightly at all speeds.

5. The addition of roughness to the first 5 percent of the airfoil chord on both upper and lower surfaces generally reduced slightly both the flap effectiveness and hinge moments due to deflection.

Langley Aeronautical Laboratory,
National Advisory Committee for Aeronautics,
Langley Field, Va.

REFERENCES

1. Johnson, Harold I.: Measurements of Aerodynamic Characteristics of a 35° Sweptback NACA 65-009 Airfoil Model With $\frac{1}{4}$- Chord Plain Flap by the NACA Wing-Flow Method. NACA RM L7F13, 1947.

2. Johnson, Harold I., and Brown, B. Porter: Measurements of Aerodynamic Characteristics of a 35° Sweptback NACA 65-009 Airfoil Model With $\frac{1}{4}$- Chord Horn-Balanced Flap by the NACA Wing-Flow Method. NACA RM L9B23a, 1949.

3. Johnson, Harold I., and Brown, B. Porter: Measurements of Aerodynamic Characteristics of a 35° Sweptback NACA 65-009 Airfoil Model With $\frac{1}{4}$- Chord Bevelled-Trailing-Edge Flap and Trim Tab by the NACA Wing-Flow Method. NACA RM L9K11, 1950.

4. Johnson, Harold I., and Goodman, Harold R.: Measurements of Aerodynamic Characteristics of a 35° Sweptback NACA 65-009 Airfoil Model With $\frac{1}{4}$- Chord Flap Having a 31-Percent-Flap-Chord Overhang Balance by the NACA Wing-Flow Method. NACA RM L50H09, 1950.

5. Göthert, B.: Control Effectiveness at High Subsonic Speeds. Reps. and Translations No. 72, British M.O.S. (A) Völkenrode, Feb. 1947.

6. Hemenover, Albert D., and Graham, Donald J.: Influence of Airfoil Trailing-Edge Angle and Trailing-Edge-Thickness Variation on the Effectiveness of a Plain Flap at High Subsonic Mach Numbers. NACA RM A51C12a, 1951.

7. Drake, Hubert M., and Carden, John R.: Elevator-Stabilizer Effectiveness and Trim of the X-1 Airplane to a Mach Number of 1.06. NACA RM L50G20, 1950.

8. Rathert, George A., Jr., Hanson, Carl M., and Rolls, L. Stewart: Investigation of a Thin Straight Wing of Aspect Ratio 4 by the NACA Wing-Flow Method.- Lift and Pitching-Moment Characteristics of the Wing Alone. NACA RM A8L20, 1949.

9. Goodson, Kenneth W., and Morrison, William D., Jr.: Aerodynamic Characteristics of a Wing With Unswept Quarter-Chord Line, Aspect Ratio 4, Taper Ratio 0.6, and NACA 65A006 Airfoil Section. Transonic-Bump Method. NACA RM L9H22, 1949.

10. DeYoung, John, and Harper, Charles W.: Theoretical Symmetric Span Loading at Subsonic Speeds for Wings Having Arbitrary Plan Form. NACA Rep. 921, 1948.

[redacted]

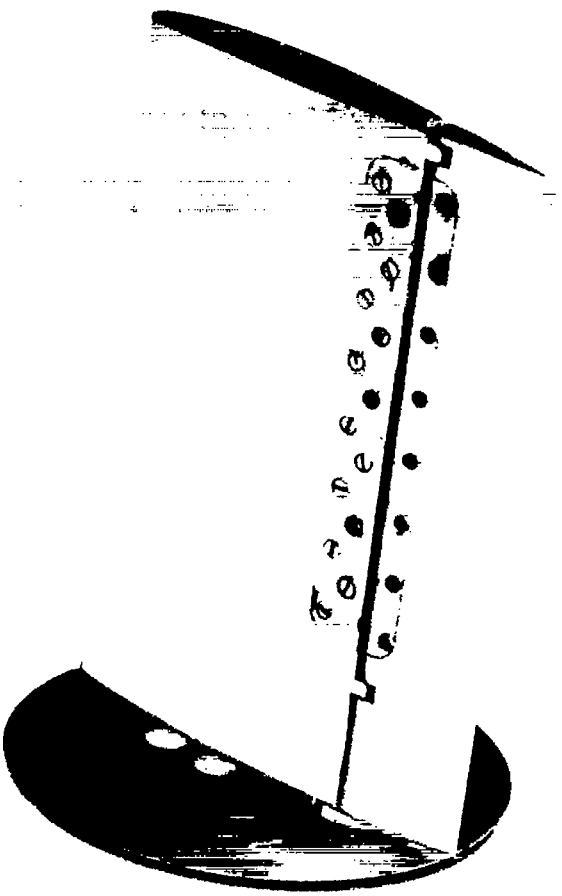

NACA
-5066.1

Figure 1.- Photograph of unswept NACA 65-009 wing-flow model with 1/4-chord full-span plain flap.

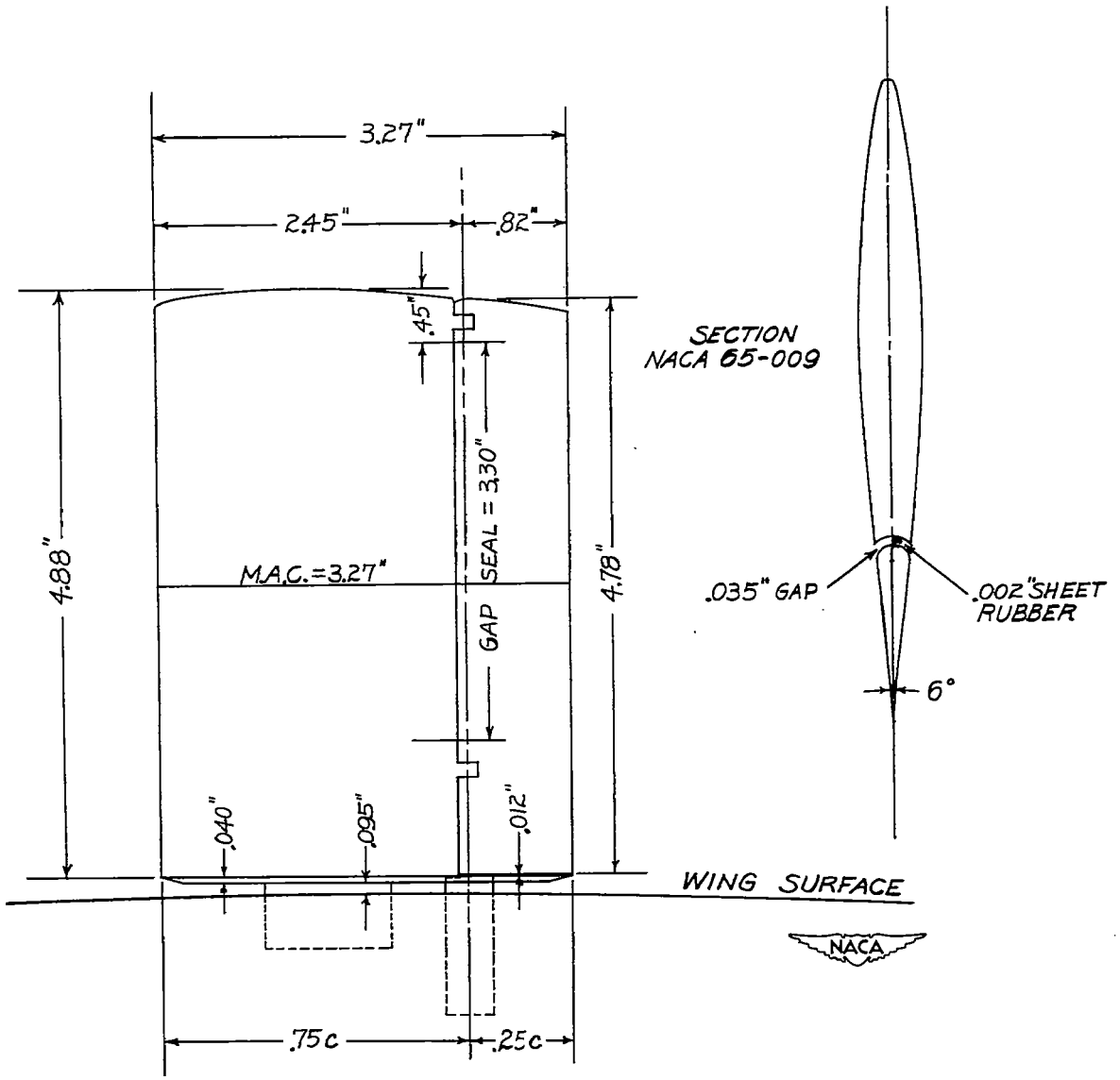

Figure 2.- Drawing of unswept semispan airfoil model with 1/4-chord full-span plain flap. Model area, 15.80 sq in.; flap area, 3.88 sq in.; aspect ratio, 3.01.

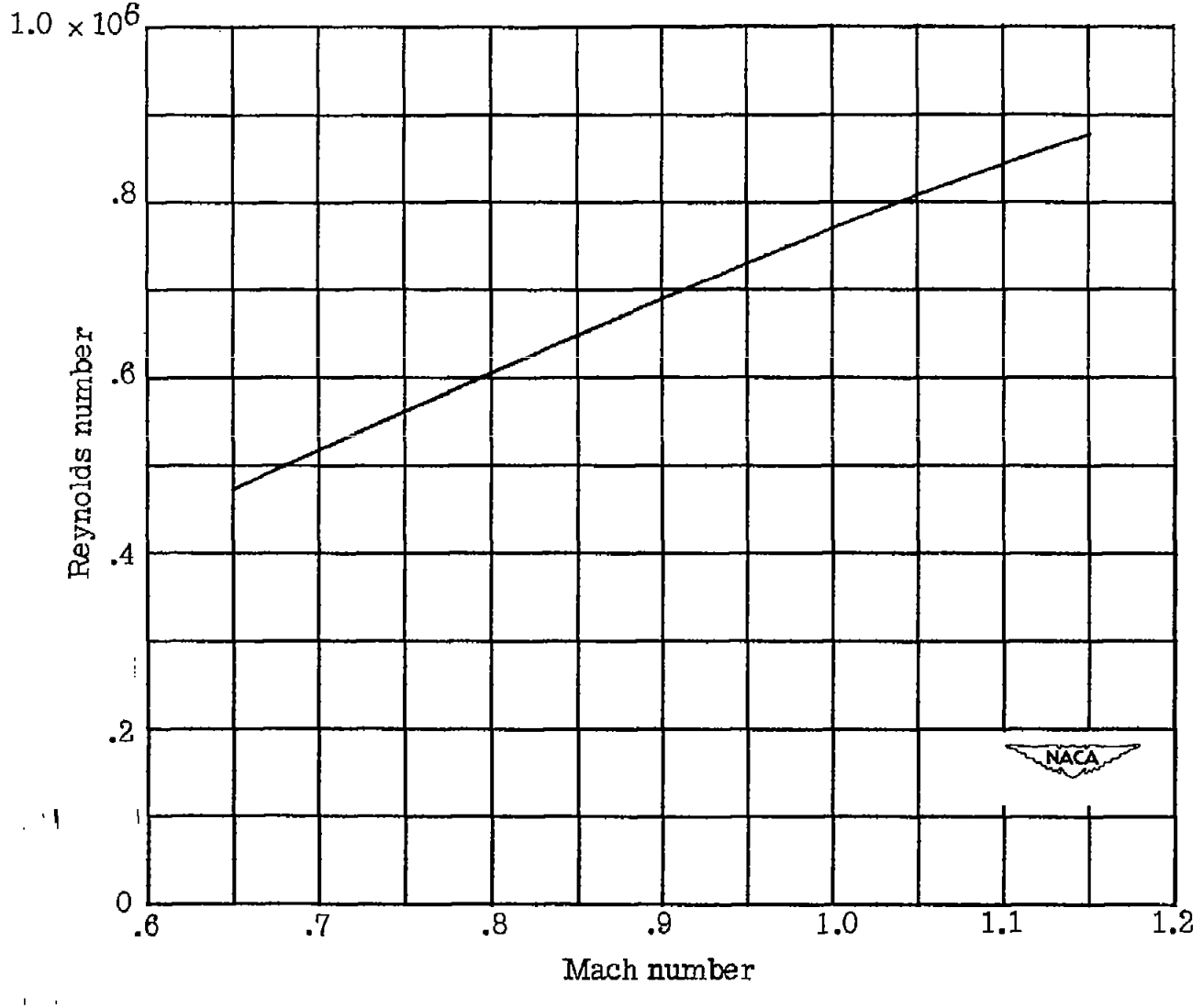

Figure 3.- Variation of Reynolds number with Mach number.

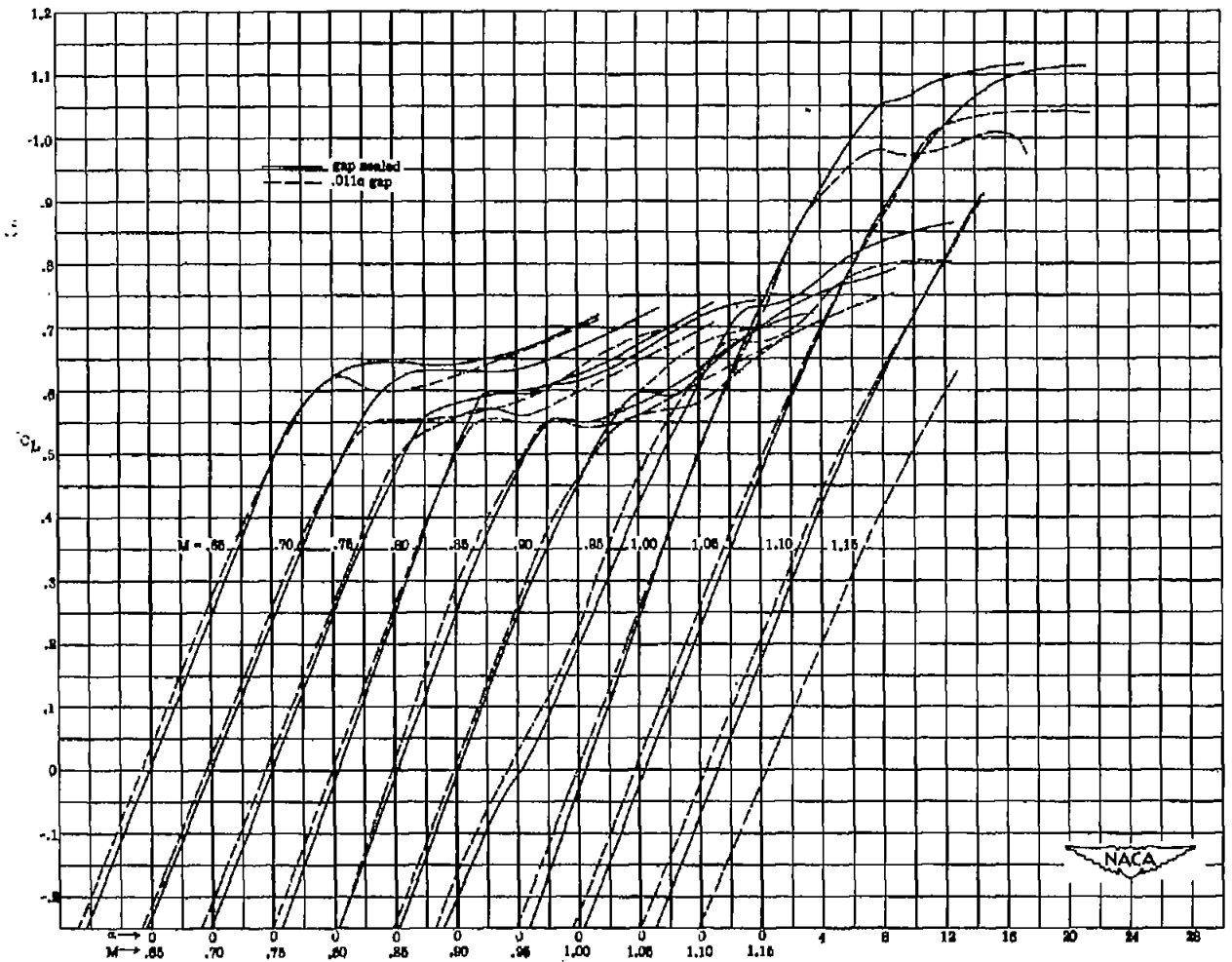

(a) Variation of C_L with α.

Figure 4.- Aerodynamic characteristics due to angle of attack throughout test Mach number range. $\delta = 0^{\circ}$.

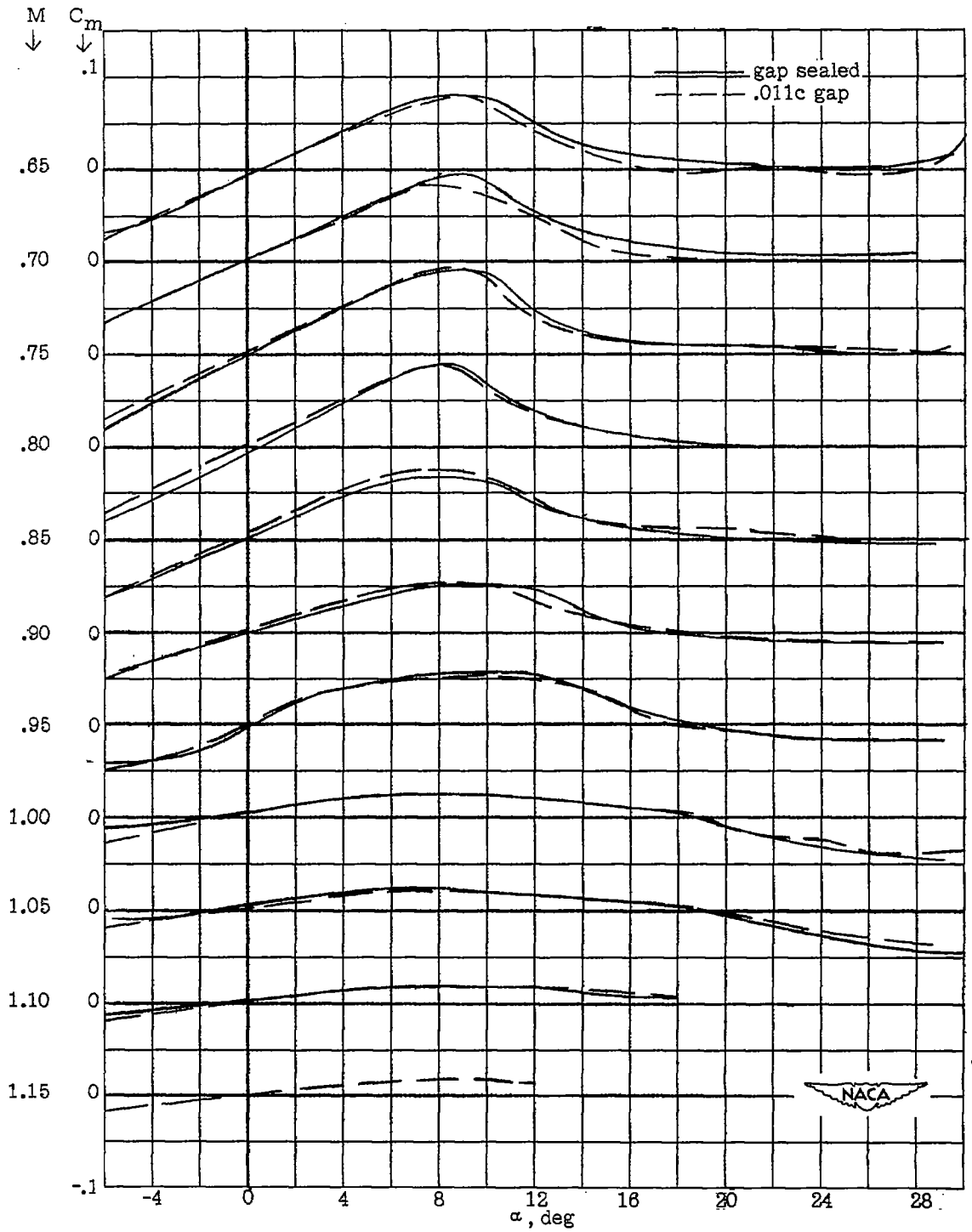

(b) Variation of C_m with α.

Figure 4.- Continued.

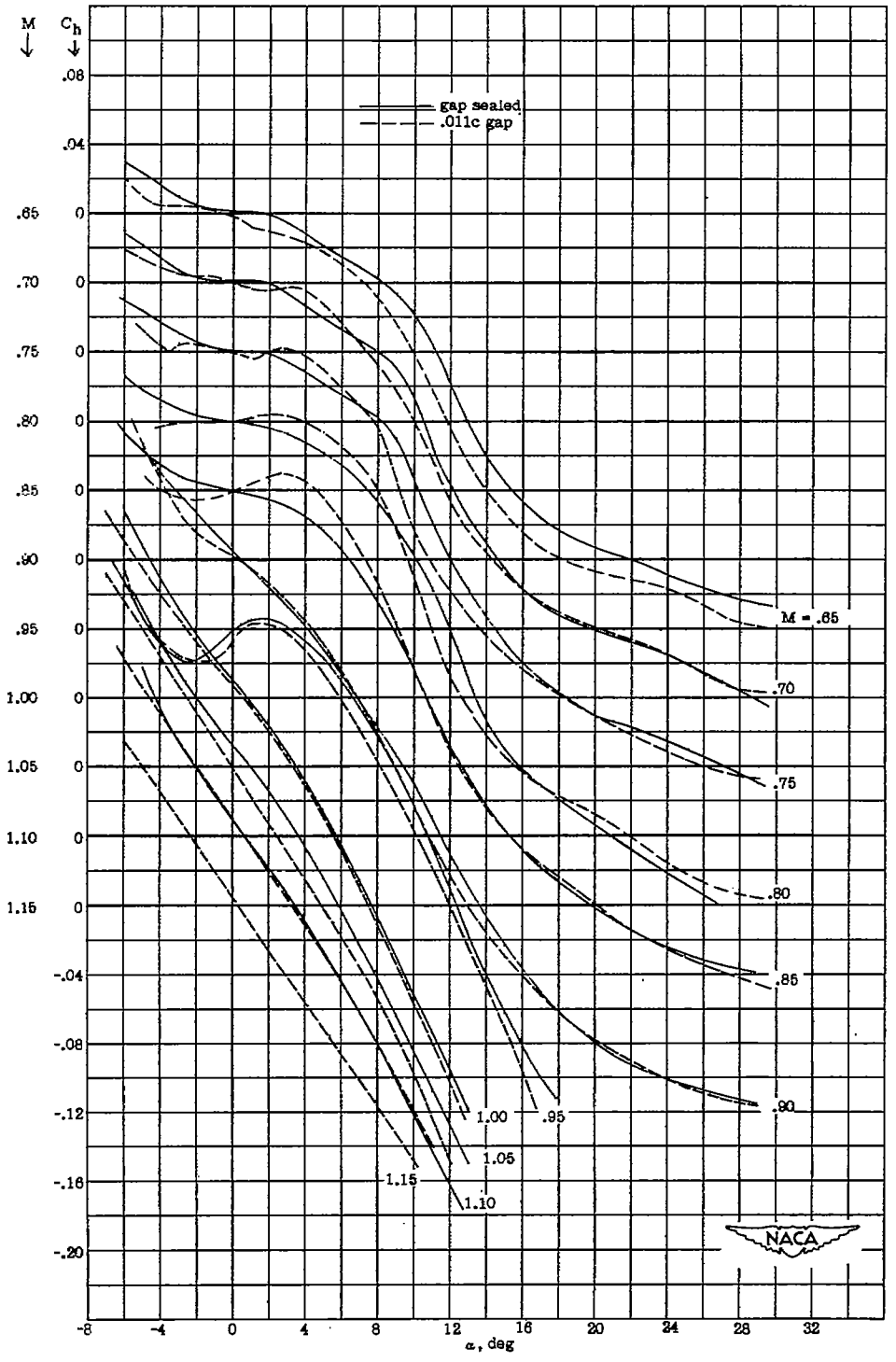

(c) Variation of C_h with α.

Figure 4.- Concluded.

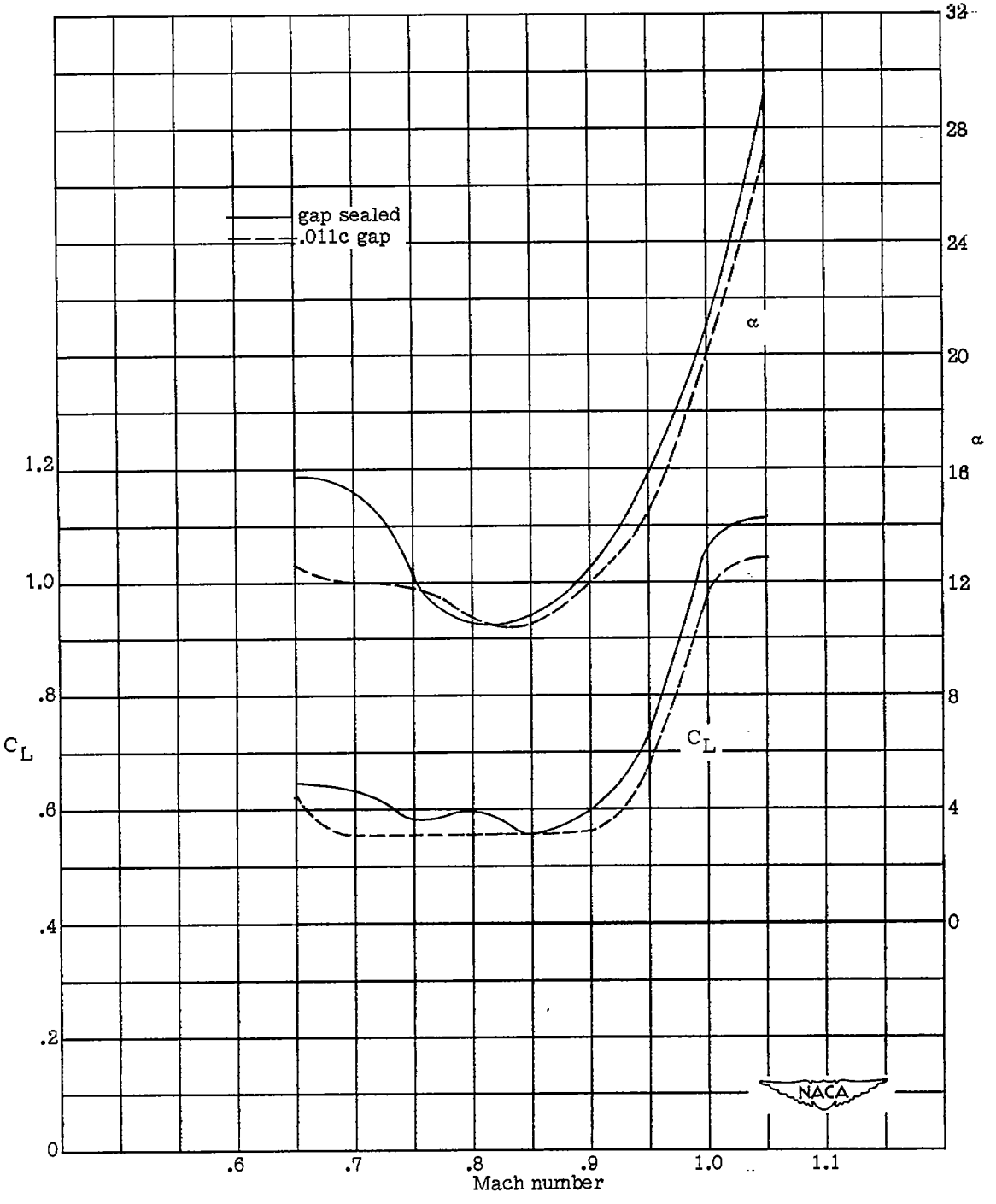

Figure 5.- Variation with Mach number of approximate lift coefficient and corresponding angle of attack at which flow breakdown occurred (approximate maximum usable lift coefficient).

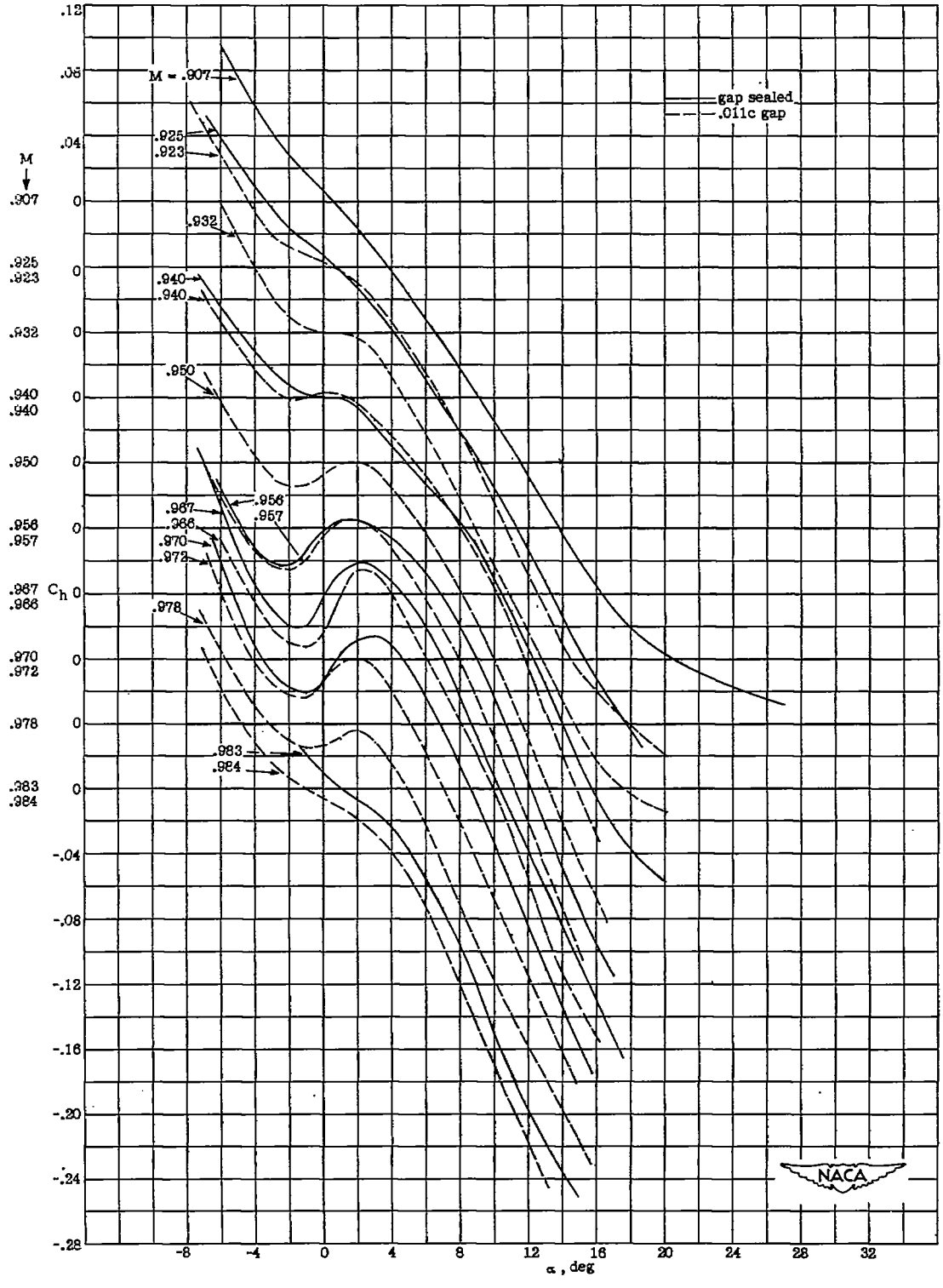

Figure 6.- Variations of hinge-moment coefficient with angle of attack for Mach numbers between 0.9 and 1.0. $\delta = 0^{\circ}$.

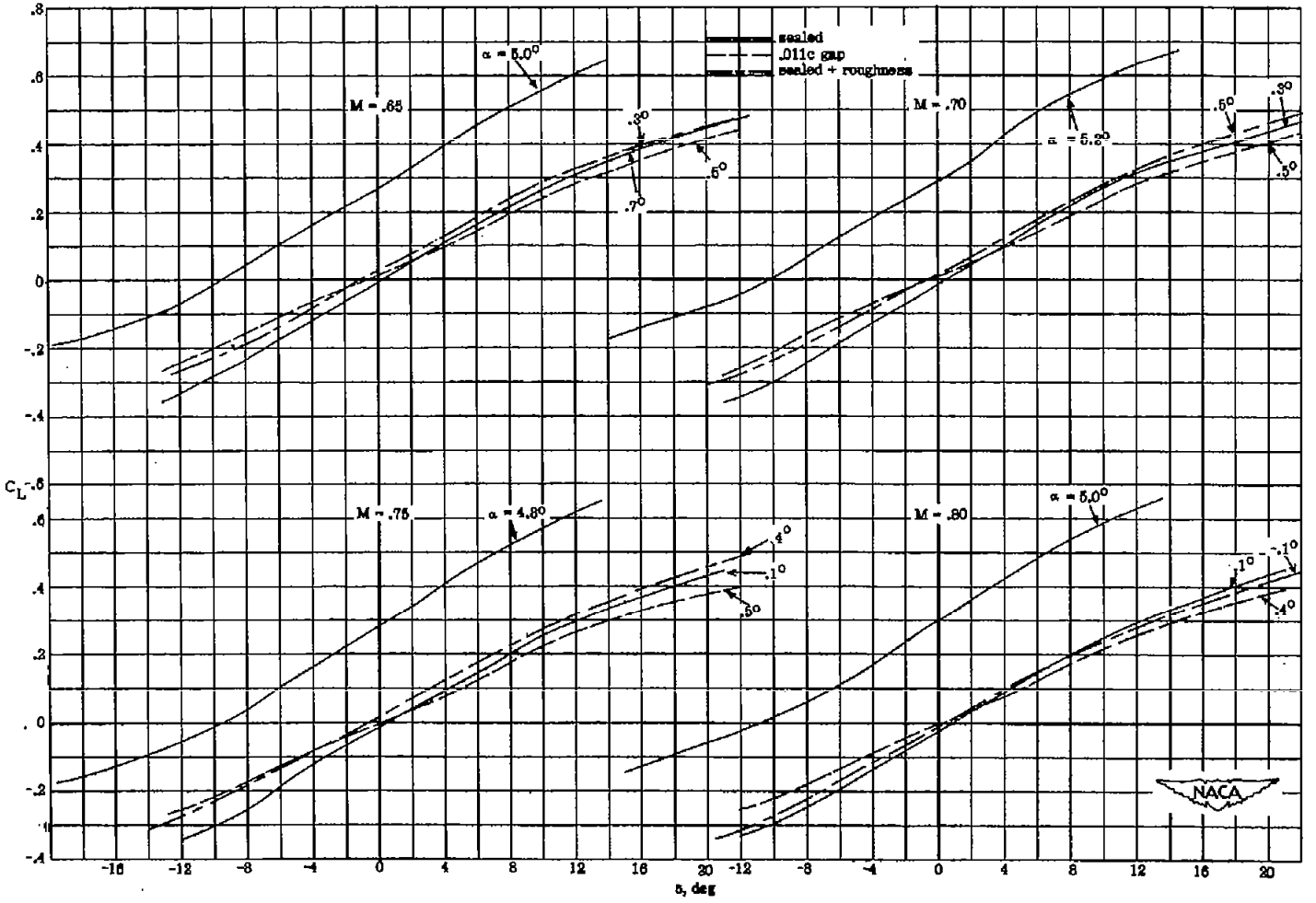

(a) Variation of C_L with δ. M = 0.65, 0.70, 0.75, and 0.80.

Figure 7.- Aerodynamic characteristics due to flap deflection throughout Mach number range.

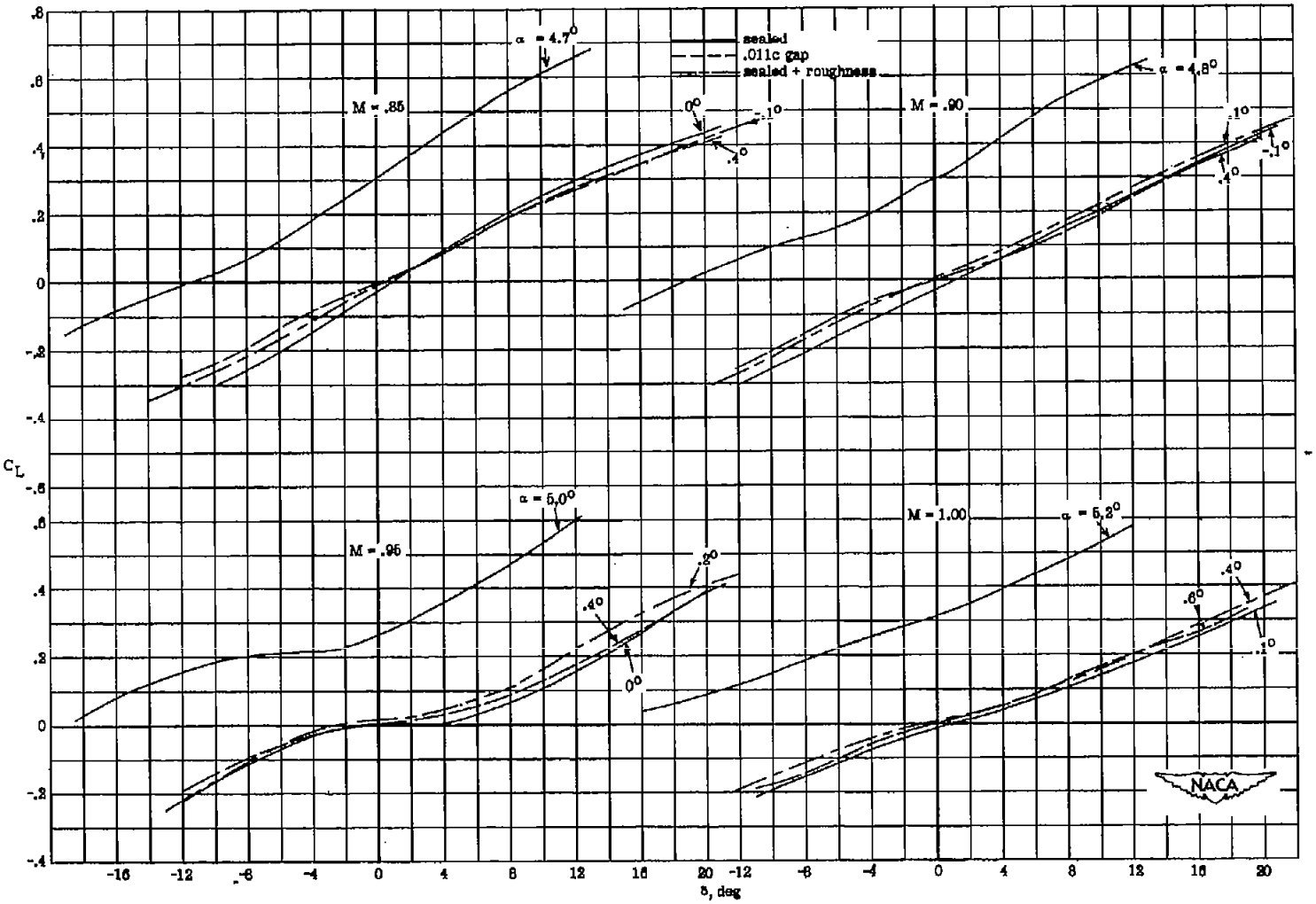

(a) Continued. M = 0.85, 0.90, 0.95, and 1.00.

Figure 7.- Continued.

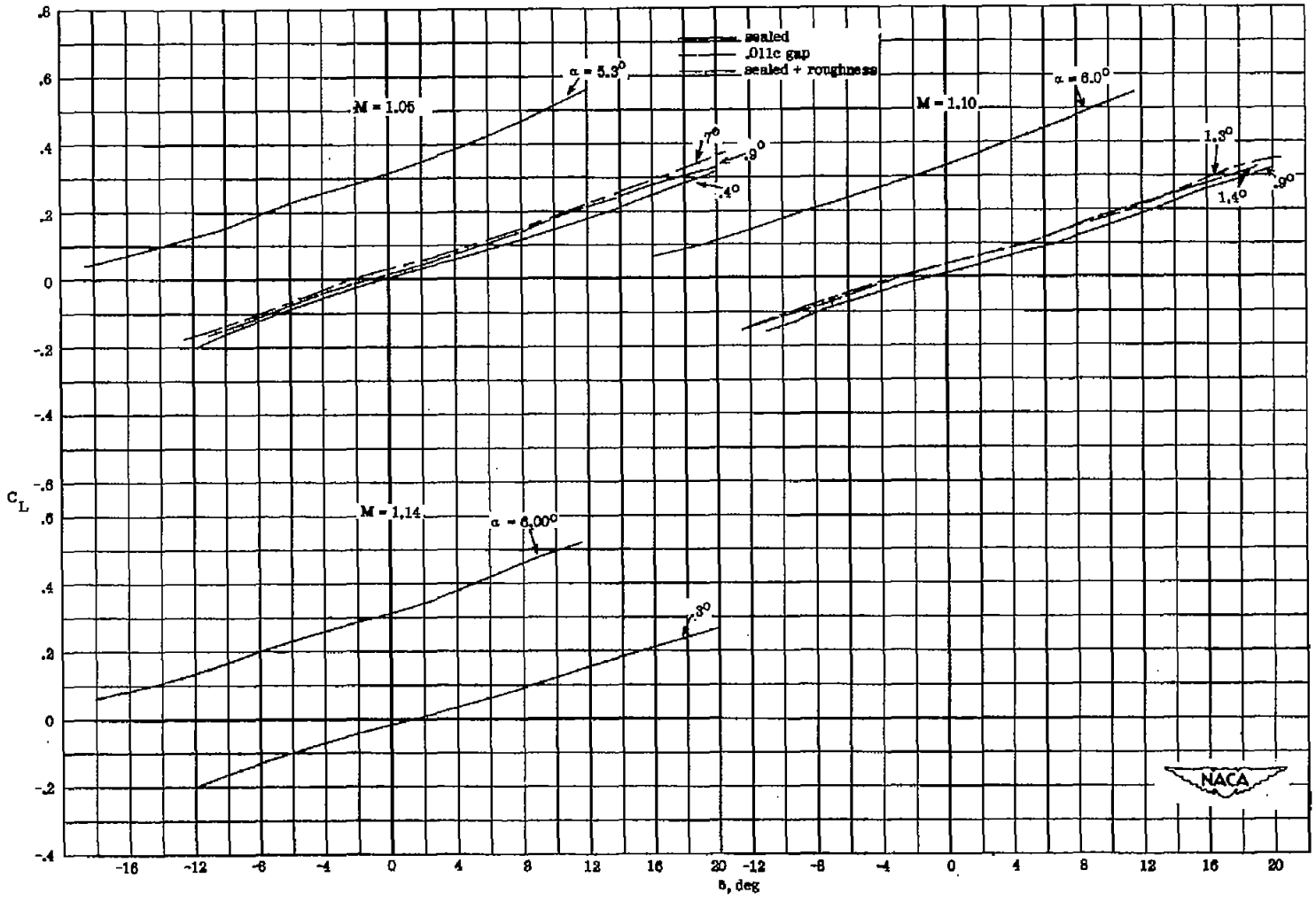

(a) Concluded. M = 1.05, 1.10, and 1.14.

Figure 7.- Continued.

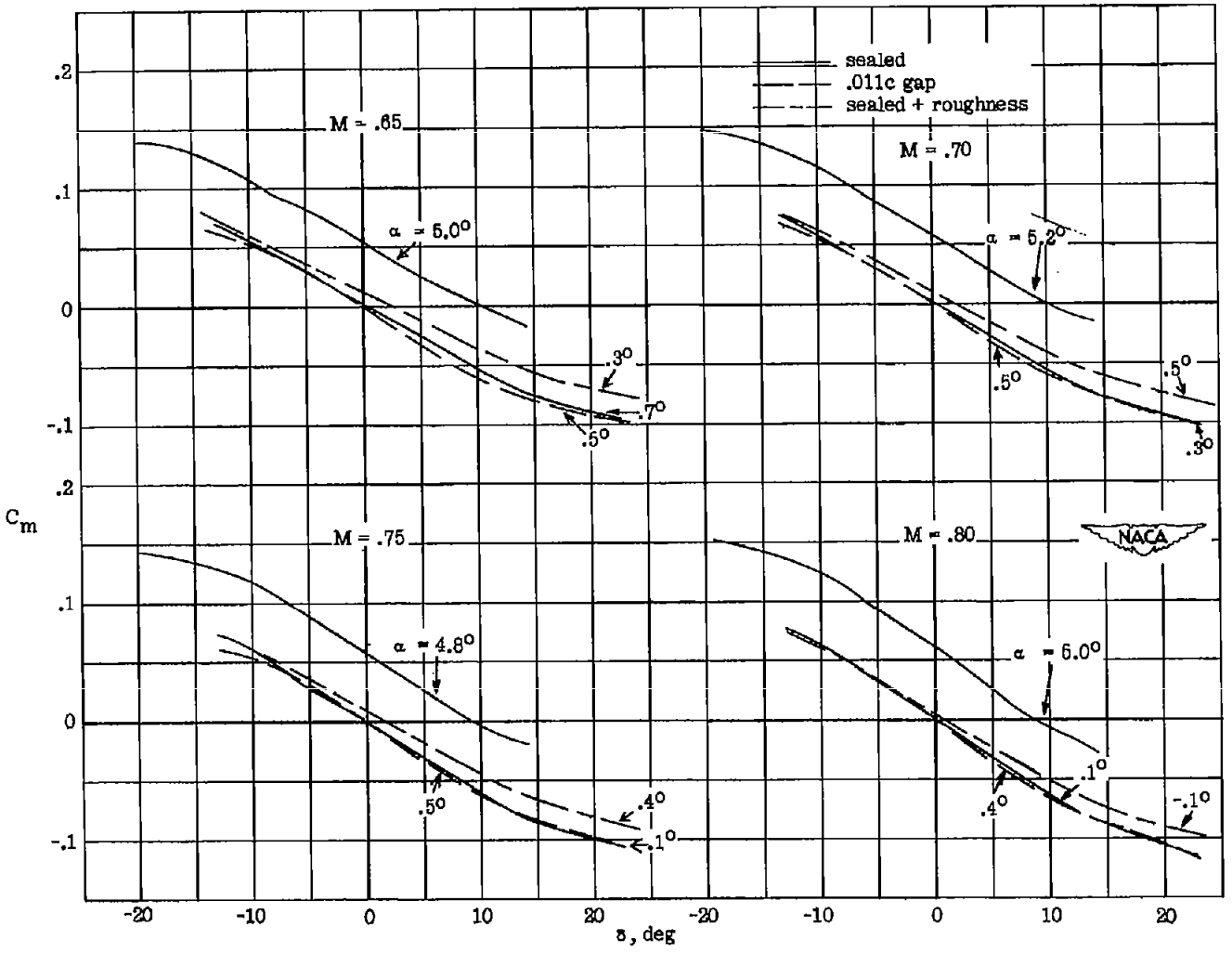

(b) Variation of C_m with δ. M = 0.65, 0.70, 0.75, and 0.80.

Figure 7.- Continued.

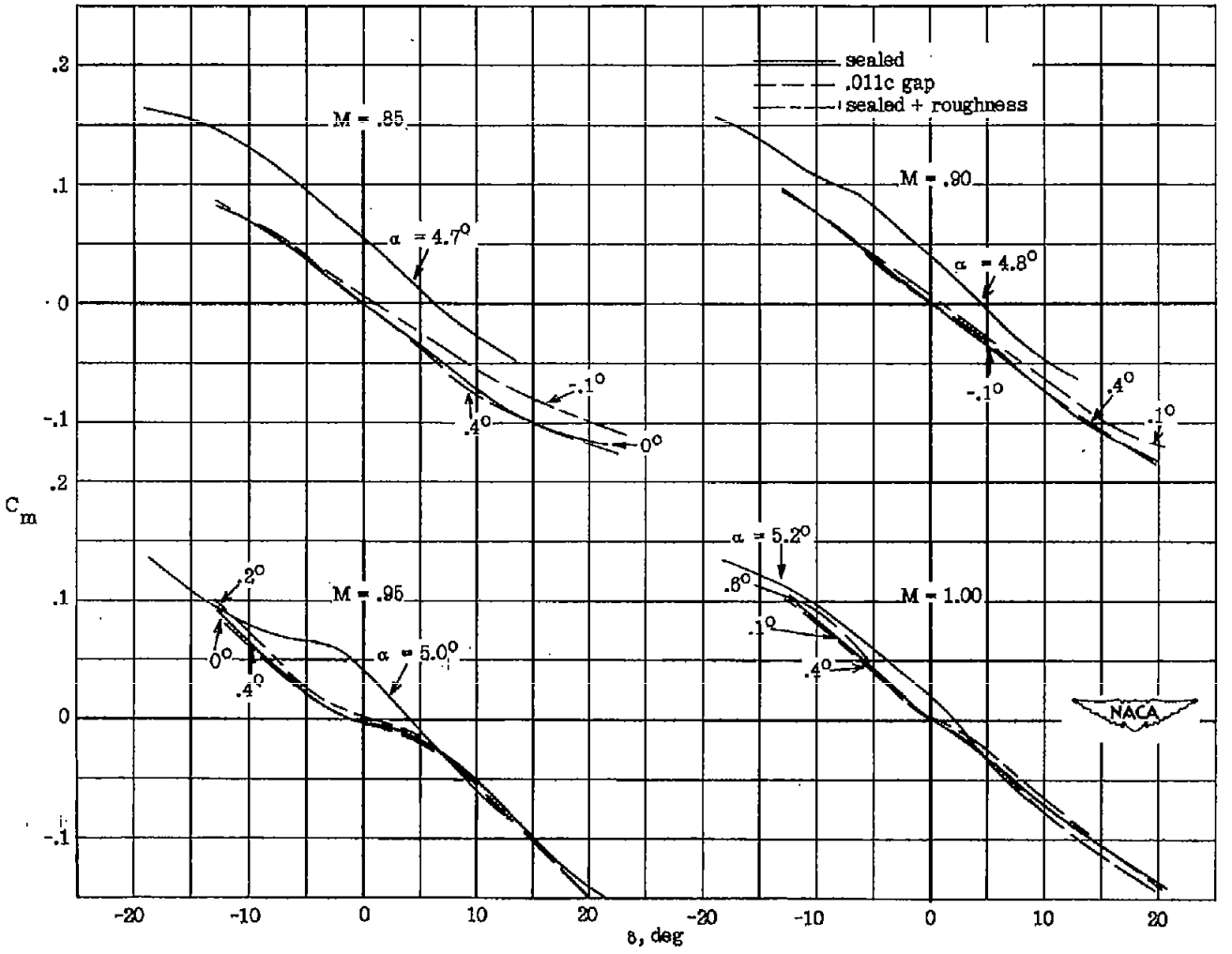

(b) Continued. M = 0.85, 0.90, 0.95, and 1.00.

Figure 7.- Continued.

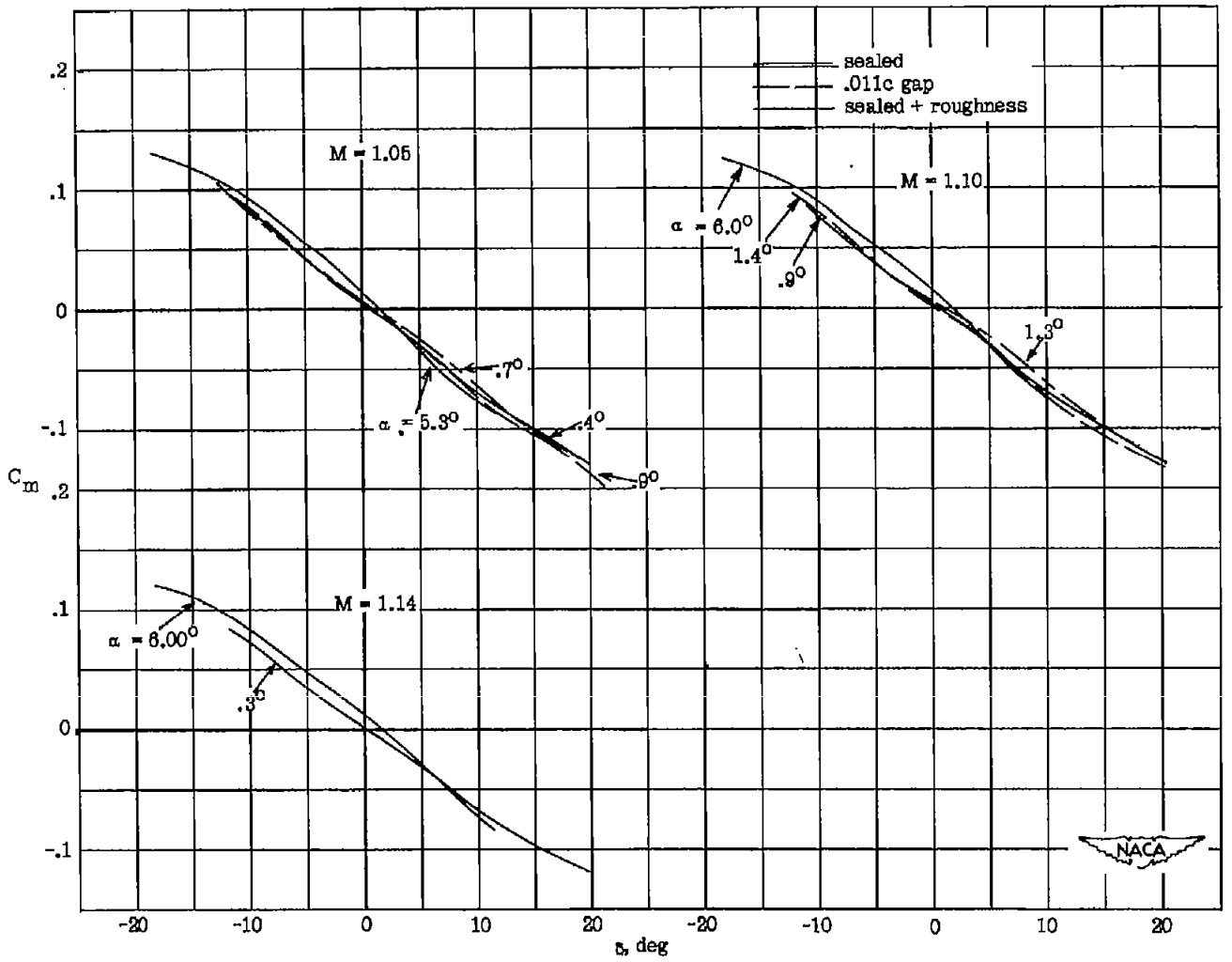

(b) Concluded. M = 1.05, 1.10, and 1.14.

Figure 7.- Continued.

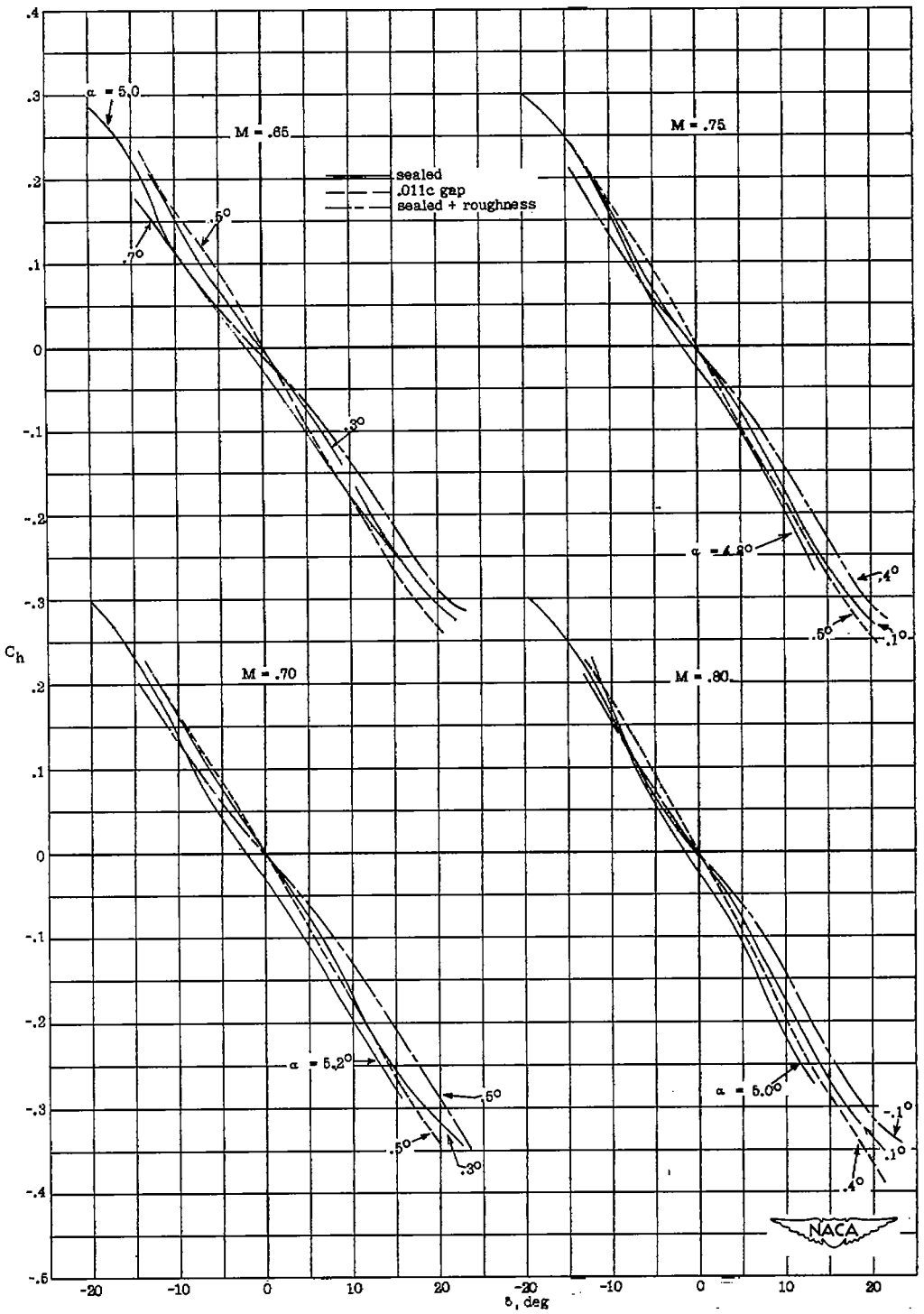

(c) Variation of C_h with δ. M = 0.65, 0.70, 0.75, and 0.80.

Figure 7.- Continued.

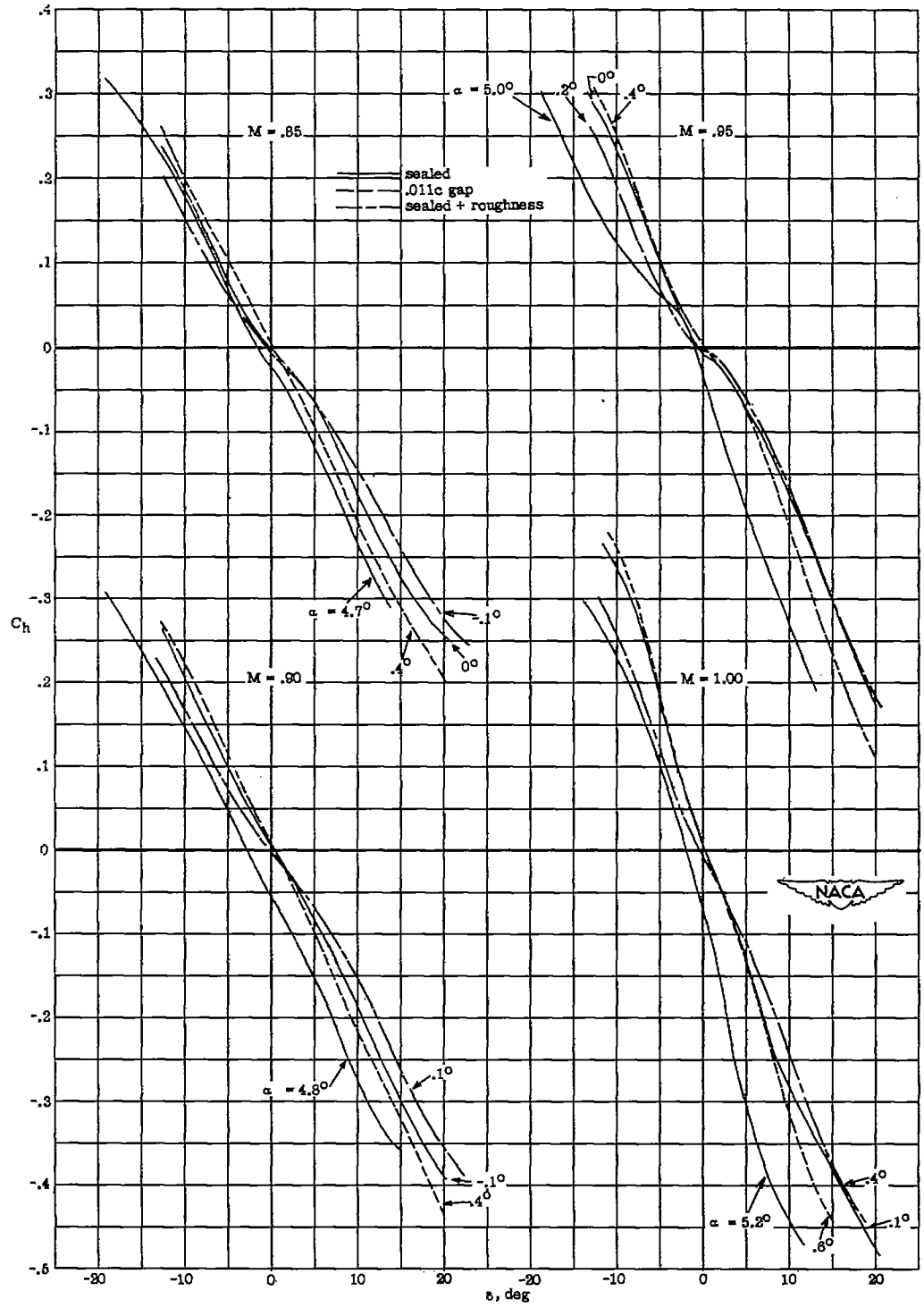

(c) Continued. M = 0.85, 0.90, 0.95, and 1.00.

Figure 7.- Continued.

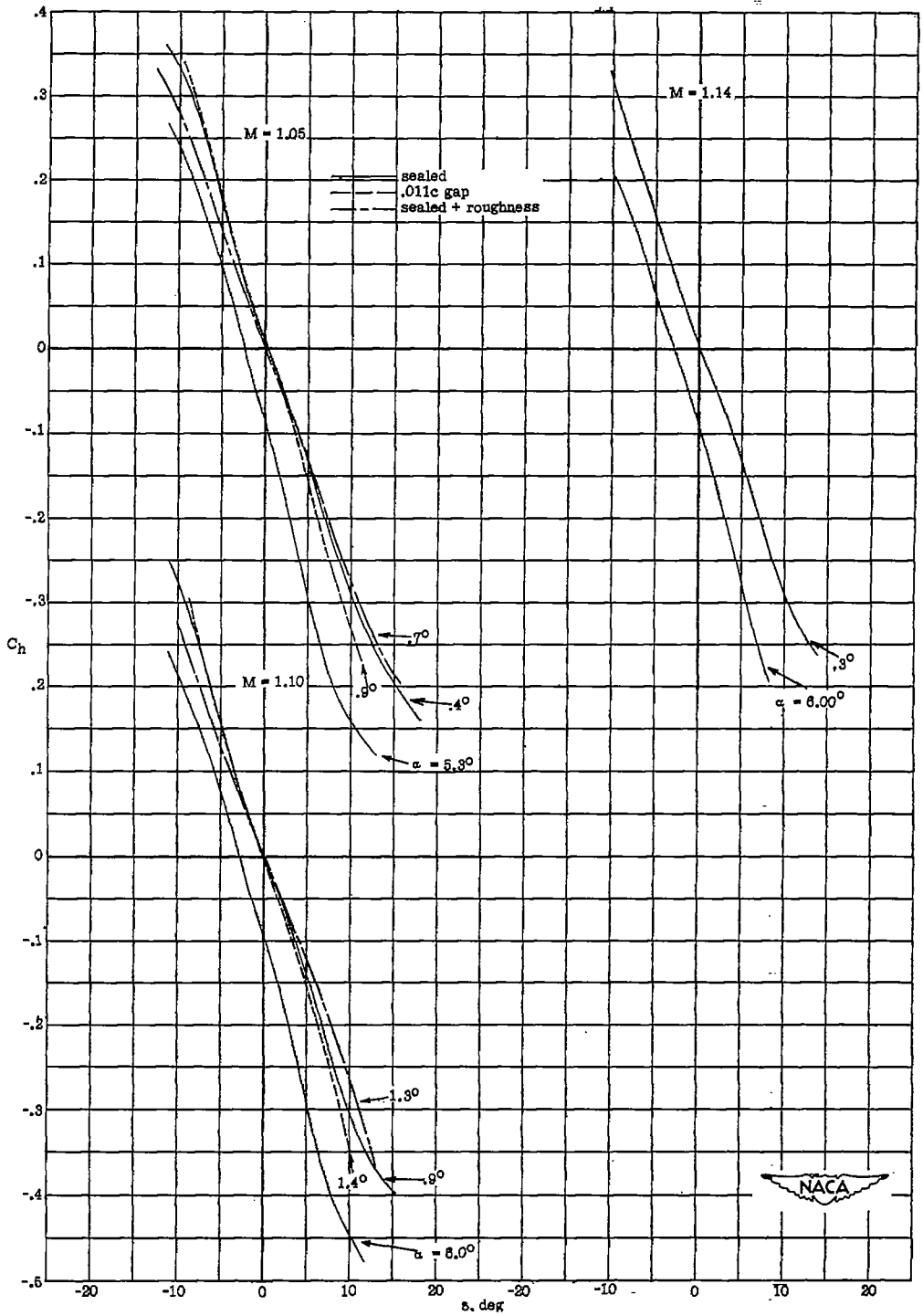

(c) Concluded. M = 1.05, 1.10, and 1.14.

Figure 7.- Concluded.

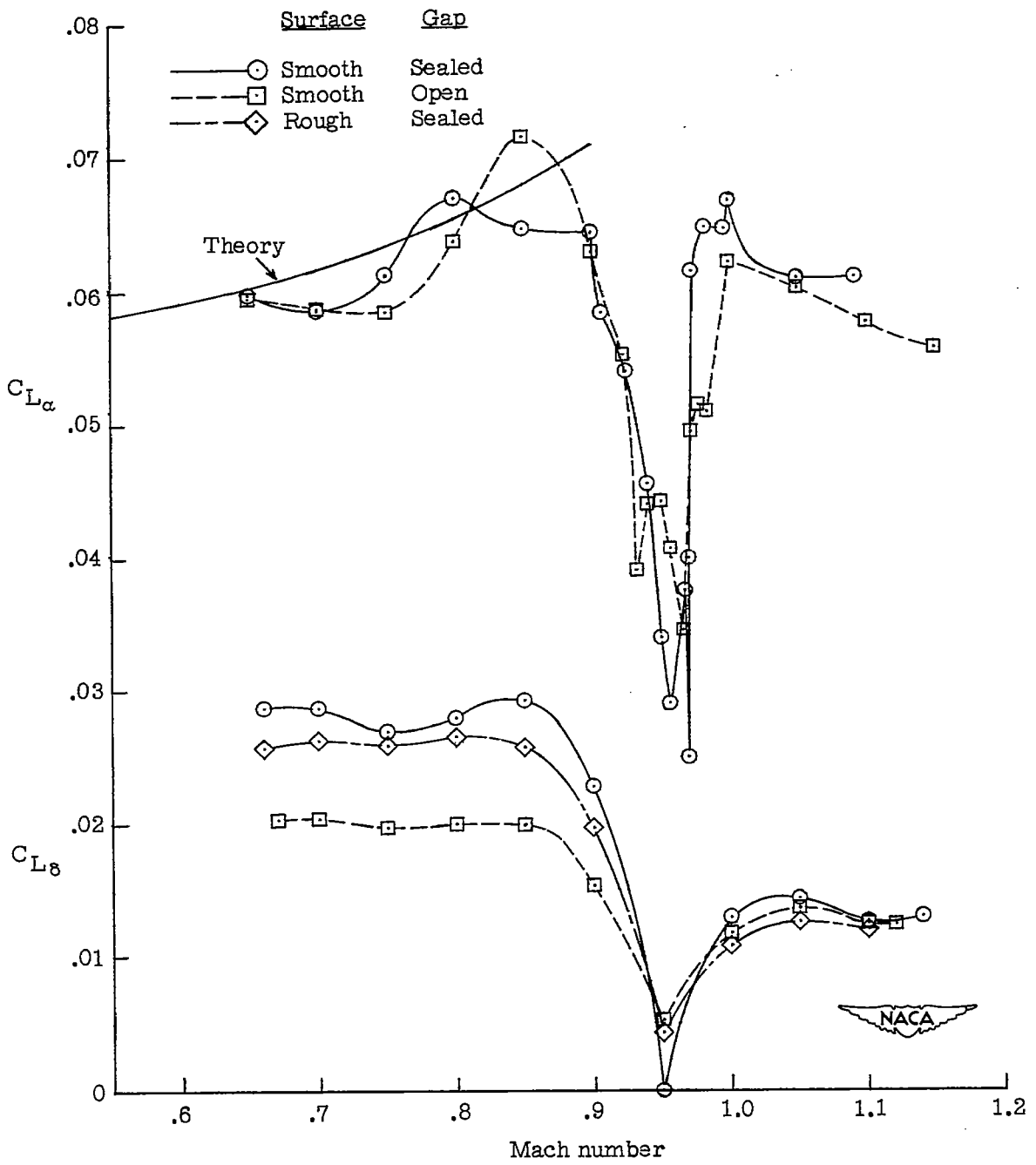

(a) Variation of C_{L_α} and C_{L_δ} with M.

Figure 8.- Summary of aerodynamic characteristics at 0° angle of attack and 0° flap deflection.

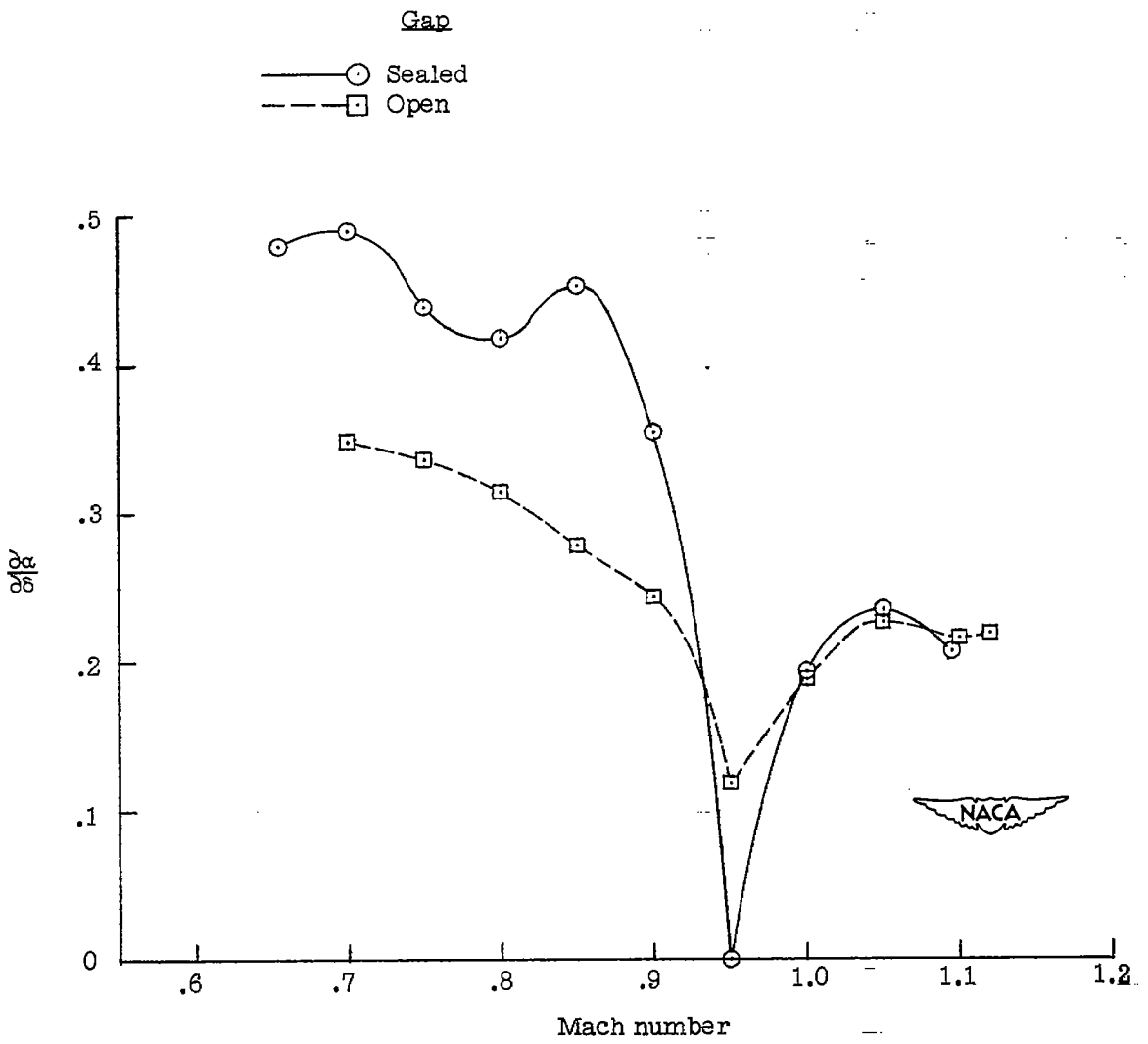

(b) Variation of $\partial\alpha/\partial\delta$ with M.

Figure 8.- Continued.

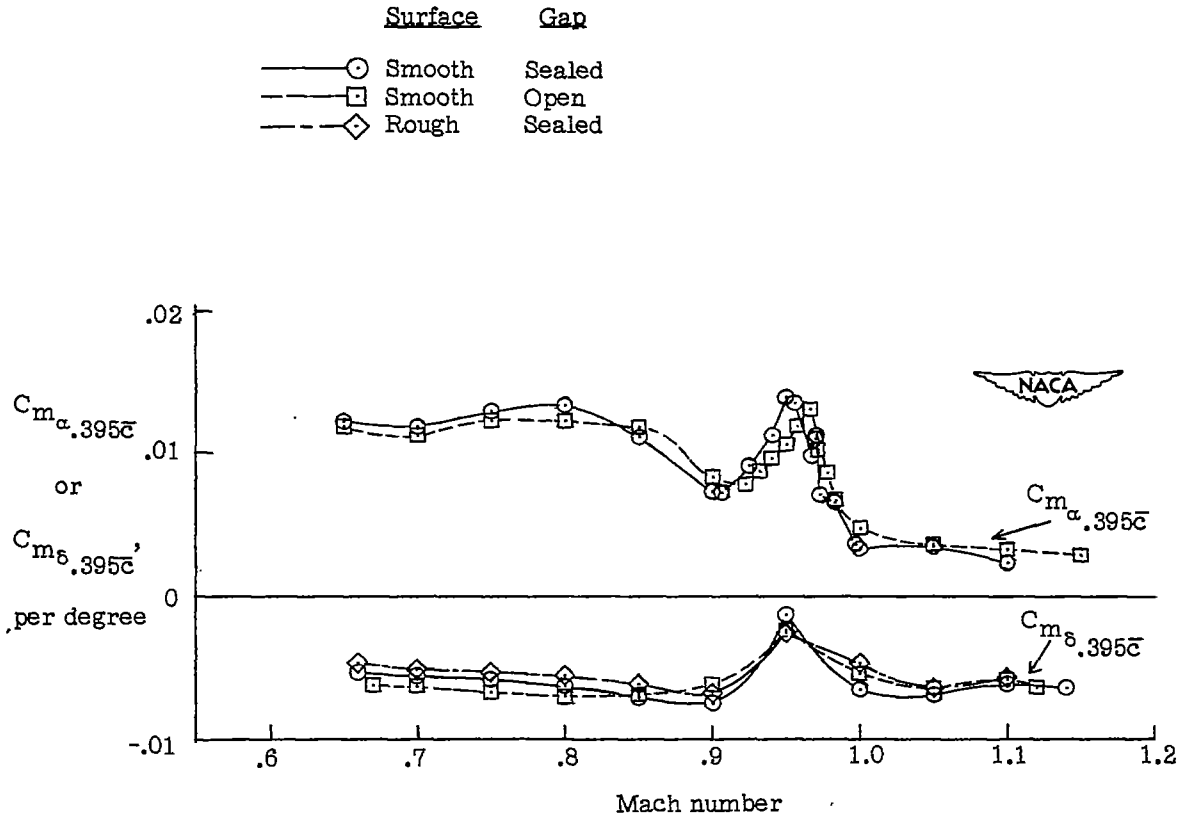

(c) Variation of $C_{m_{\alpha_{0.395\bar{c}}}}$ and $C_{m_{\delta 0.395\bar{c}}}$ with M.

Figure 8.- Continued.

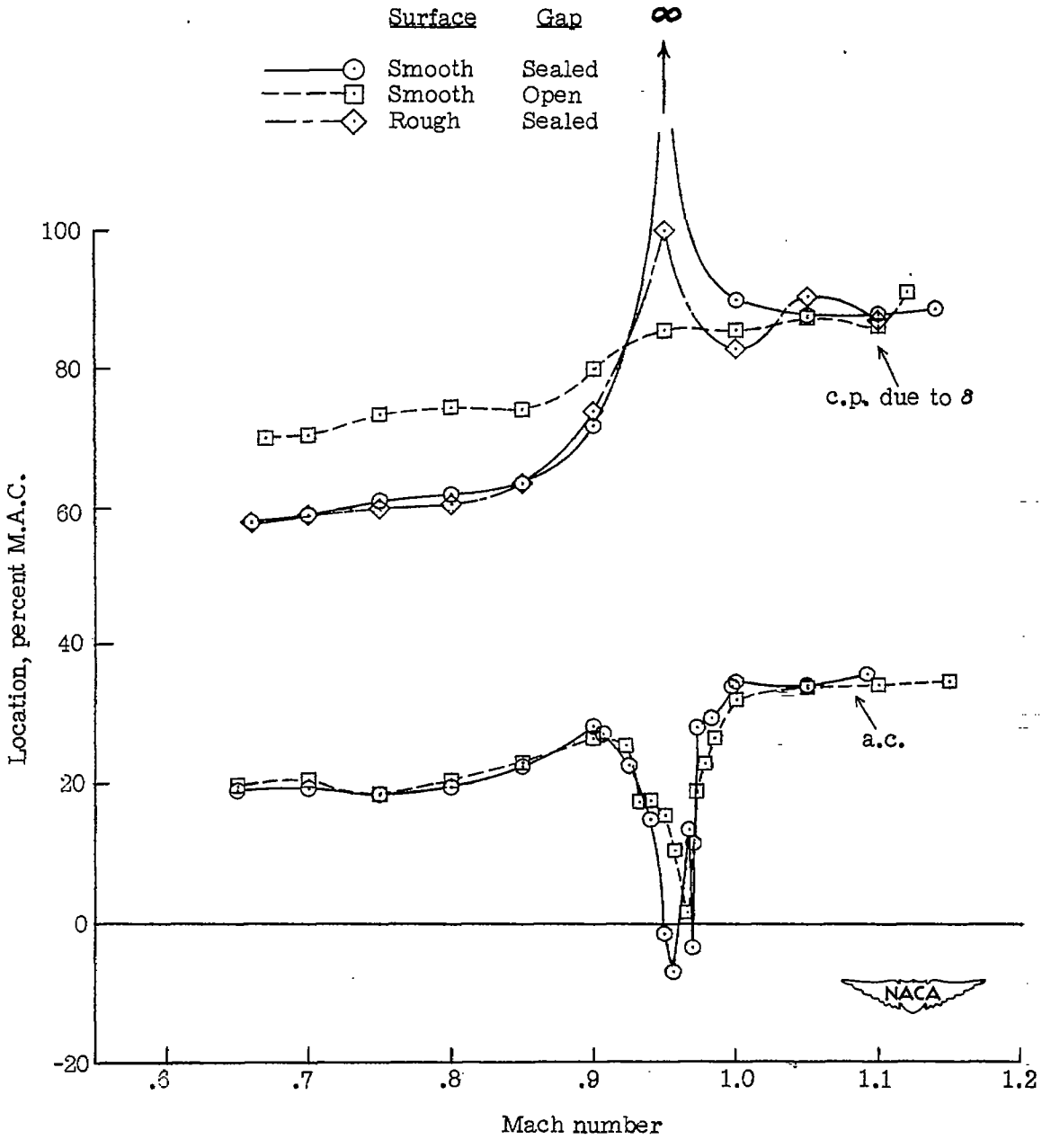

(d) Position of aerodynamic center and center of pressure due to flap deflection plotted against Mach number.

Figure 8.- Continued.

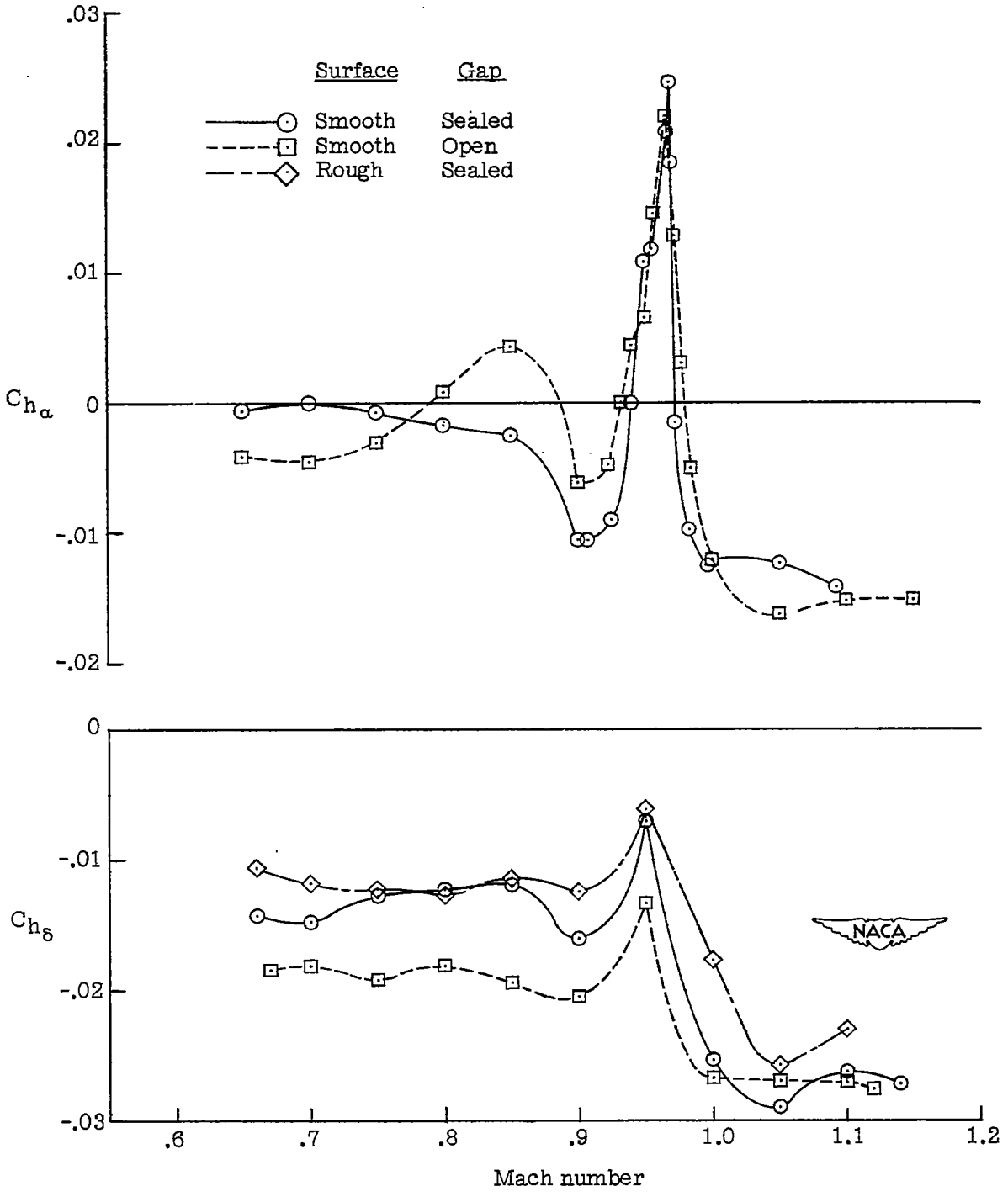

(e) Variation of C_{h_α} and C_{h_δ} with M.

Figure 8.- Concluded.

NACA-Langley - 6-10-53 -325